Moscow University Physics Bulletin
Vol. 55, No. 2, pp. 35–40, 2000

Vestnik Moskovskogo Universiteta. Fizika
UDC 621.385.833:628.94

STUDYING THE EFFICIENCY OF SCINTILLATION DETECTORS FOR BACK-SCATTERED ELECTRONS IN SEM

R. N. Birchenko, E. I. Rau, and M. N. Filippov

The experimental investigations conducted have shown that the scintillation detectors used in scanning electron microscopy for the registration of back-scattered electron fluxes differ noticeably in the efficiency of detection by different regions of their active part.

Scintillation detectors for electrons of moderate energies (1–50 keV) have found wide application in nuclear physics, cosmic ray physics, and electron microscopy. In scanning electron microscopy (SEM), scintillation detectors are used to register the back-scattered electron flux with a view to forming an electron-microscopic image under electron back scattering conditions [1–5].

PROBLEM FORMULATION AND EXPERIMENT STAGING

To experimentally verify the fact that there are significant differences in the efficiency of detection of back-scattered electrons between different regions of the active part of scintillation detectors, comparison was made between the characteristics of back-scattered electron detectors differing in geometric shape and a ring-shaped semiconductor detector. The configurations of the optical part of the scintillation detectors studied are presented in Fig. 1. Figure 1*a* schematically shows the optical part of the Robinson scintillation back-scattered electron detector [6] that is most widely used in commercial SEMs. The detector body is a prism whose lower face (the active part of the detector) makes an angle of 7 deg with the upper face and has a rectangular shape. The light guide is connected to the wider vertical face of the prism. All surfaces, save for the active part, are metallized. The commercially available detectors measure 97 mm by 30 mm (with reference to the upper face), the height of the smaller, vertical face is 2 mm. Figure 1*b* is a cross-sectional view of the Robinson detector modification suggested by us. Widely applied in SEM are also ring-shaped back-scattered electron detectors, both semiconductor and scintillation types [7]. The configuration of the active part of such a detector is shown in Fig. 1*c*.

The detectors being studied were mounted in the standard place under the SEM objective lens, at a distance to the sample of 10–15 mm. Optical radiation was coupled out by means of a light guide of special shape that smoothly connected together the optical part of the detector and the photomultiplier.

The test object used was a metal ball 1 mm in diameter. By varying the position of the electron probe aimed at a certain spot on the spherical surface, one can vary the position of the maximum of the back-scattered electron directivity diagram so as to scan this diagram along an arbitrary line on the surface of the detector active part [8]. In that case, the output signal from the detector will be proportional to the convolution of the local detection efficiency function with the angular and energy distributions of back-scattered electrons.

The scanning was effected along one of the axes of a rectangular coordinate system located in the plane of the detector active part and directed along the diameters of the ring-shaped detector (one of the axes passed in that case through the light guide coupling region and the center of the detector active part and the other, perpendicular to the former, through the center of the detector). The relevant relationships

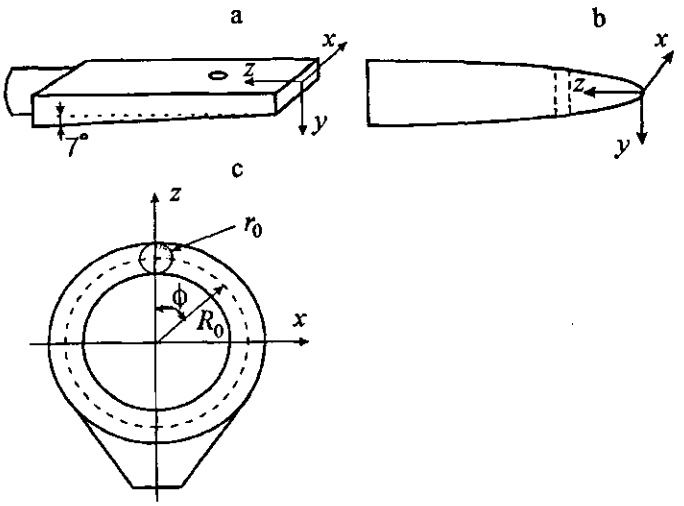

Fig. 1

Shape of the optical part of the scintillation back-scattered electron detectors studied: (*a*) Robinson detector; (*b*) scintillation detector in the shape of an elliptic paraboloid; (*c*) ring-shaped detector.

for the output signal magnitude, $I_{out} = I_{out}(x)$ and $I_{out} = I_{out}(y)$, are presented in Fig. 2. Curves *1* and *3* refer to the ring-shaped scintillation detector, curves *3* and *1* being respectively obtained when scanning along the axis passing through the light guide coupling region and the perpendicular axis. Curve *2* refers to the semiconductor detector; its shape is independent of the orientation of the scanning line passing through the center of the detector active part. Curve *3* is highly asymmetric, its maximum being shifted toward the active part regions adjacent to the exit light guide.

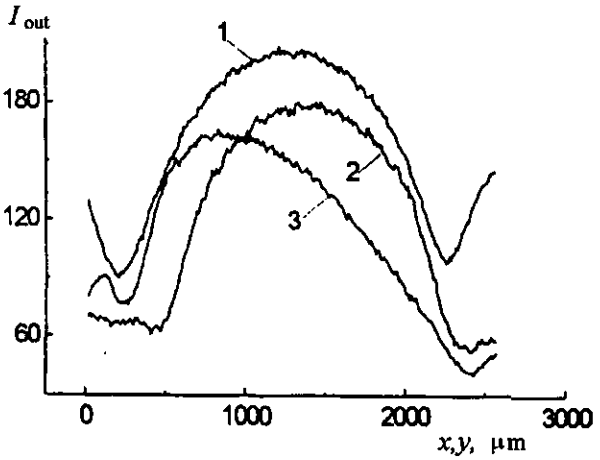

Fig. 2

Output signal I_{out} (in relative units) of the ring-shaped back-scattered electron (curves *1* and *3*) and the semiconductor (curve *2*) detector for various scanning directions: scanning along the axis passing through the light guide coupling region (curve *3*) and along the perpendicular axis (curve *1*).

The asymmetry observed in curve *3* can be explained by the fact that the loss of optical radiation in the course of its propagation from the generation region to the photodetector is higher for those regions of the detector active part which are located farther away from the exit light guide. This conclusion is

borne out by the complete symmetry of the output signal curve for the semiconductor detector (curve *2*), for in this detector there is no process similar to the light transport in the scintillation detector. When the scanning line orientation is along the Ox-axis in the case of scintillation detector, the light transport conditions for regions located at equal distances from the detector center will be the same. In that case, the scintillation detector output signal curve should be symmetrical as is experimentally observed (curve *1*).

The results presented show that the efficiency of detection of the back-scattered electron flux in the scintillation detectors actually used in SEM is perceptibly nonuniform in different regions of the active part. The quantitative methods using back-scattered electron detection require the knowledge of the local transformation function of the detector at all points of its active part surface. This function characterizes the efficiency of the light transport from the generation site to the exit from the optical system. The experimental method used above cannot help to determine this function at the necessary intervals because of the substantial angular width of the directivity diagram of back-scattered electrons. The form of this function can be investigated in more detail by using focused electron beams to effect local generation of optical radiation. To this end, use can be made of the SEM electron probe. The scintillation detector to be studied is placed, with the light guide attached, on the microscope stage so that its electron probe can be aimed at various regions of the active part. We used this technique to experimentally verify the correctness of the theoretical model presented below for the light transport in the scintillation detector.

In the general case, to experimentally determine the above-mentioned transformation function is a fairly complicated problem. We have therefore developed a theoretical model allowing the desired scintillation detector characteristics to be calculated. The loss of radiation in the light transport through the optical part of the scintillation detector is due to two factors: the radiation absorption by the detector optical part material and the escape of some radiation through the system side faces. With the materials used at present, the light scattering effect can be disregarded.

Depending on its design on the surface of the scintillation detector optical part there can take place the following three processes: simple reflection without any change in intensity in the metallized regions of the surface, refraction with partial reflection in the nonmetallized regions of the surface, and diffuse reflection from matted surfaces. The latter process is a comparatively rare occurrence in scintillation detectors, and so it will not be considered in the given model. The loss of intensity in interaction with a nonmetallized surface is described by the Fresnel formulas [9].

The analytical calculation of the scintillation detectors efficiency, i.e., the determination of the relationship between the optical radiation intensity at the exit from the system and the intensity of radiation generated in the active part, can only be carried out for symmetrical systems (see, e.g., [10, 11]). In systems with an arbitrary shape of the boundary, the calculation can only be carried out by way of consecutively tracing the rays through the optical system, with due consideration being given for the boundary conditions. This approach proved effective in calculating the characteristics of a number of scintillation detectors used in nuclear physics [12, 13] and in estimating the loss involved in the light transport in the Everheart–Thornly-type secondary electron collectors [14] used in SEM.

In our model, the generation of optical radiation is reduced to the detector active part surface. Actually the free path length of reflected electrons in the material may be as long as 10 μm. The optical part characteristic size amounts to 1–10 cm, i.e., the ratio between these quantities is 10^{-4}–10^{-5}, and so the distribution of the optical radiation sources can be considered to be of purely surface type. The angular distribution of the generated radiation within the active region is taken to be isotropic.

The calculation algorithm for the detector efficiency function D for some point $M(x, y, z)$ is as follows. The shape of the optical part of the scintillation detector is specified by a system of equations of general form, $F(x, y, z) = 0$. For the sake of definiteness, use is made of a rectangular coordinate system whose axis orientation for concrete detector configurations is presented in Fig. 1. The spatial equation of the ray passing through the starting point $M = M(x_0, y_0, z_0)$ (the point on the detector active part surface where the optical radiation source is located) has the form $(x - x_0)/m = (y - y_0)/n = (z - z_0)/k$. Here m, n, and k are the direction cosines of the ray. For the given m, n, and k, the simultaneous solution of the ray and detector surface equations defines the point $M_1 = M_1(x_1, y_1, z_1)$ at which the ray intersects the surface of the scintillation detector optical part for the first time. With x_1, y_1, z_1 calculated, the length of the first interval M_0M_1 is determined, and the intensity of the incident ray at the point M_1 is calculated with due regard for absorption. This done, the condition $I_j > 0.001$ (I_j being the ray intensity at the jth step of

the program) is checked. If this condition is not satisfied, the ray is considered to be absorbed within the optical system, and the program goes to the tracing of a new ray. If the condition is satisfied, the detector surface region corresponding to the position of this point is determined proceeding from the actual design of the detector. If the point M_1 is located on the surface of the light guide exit section, the ray is considered to have reached the photodetector, and the value of I_j is then added to the contents the output intensity counter. If the point M_1 is located in other surface areas of the scintillation detector optical part, one then determines whether this region is metallized or not, proceeding from the actual detector design. It is assumed that reflection from a metallized surface involves no change in intensity. Intensity calculations for nonmetallized surface regions are performed by the Fresnel formulas. Thereafter the procedure is repeated for the second, third, etc. intervals in the same way until one of the following events occurs: either the inequality $I_j > 0.001$ ceases to be satisfied or the position of the point on the surface at the ith step comes to correspond to the optical system exit part. The output intensity value dI_{out} for the given starting point M and N rays traced is determined as the sum of relevant partial intensities I_j, $dI_{\text{out}} = \sum I_j$. Thus, the value of the local light transport efficiency function $D(M)$ is determined by the relation $D(M) = (1/N)\sum I_j$, where $M = M(x, z)$ is the point with the coordinates x, z on the surface of the detector active part. Using this technique, one can determine the value of $D(M)$ for any arbitrary point M of the scintillation detector active part.

EXPERIMENTAL AND MATHEMATICAL MODELING RESULTS FOR LIGHT TRANSPORT IN SCINTILLATION DETECTORS

We have found the function $D = D(\varphi)$ for a ring-shaped scintillation detector, where the angle φ is reckoned from the z-axis (see Fig. 1*c*). The detector itself is a torus with a radius of $R_0 = 50$ mm and a round cross section whose radius is $r_0 = 5$ mm. The theoretical function $D = D(\varphi)$ is presented in Fig. 3 (curve *1*). The experimental function $D = D(\varphi)$ (curve *2*) is obtained in the range $\varphi = 45$–180 degs. The good agreement between the curves points to the correctness of the light transport model developed.

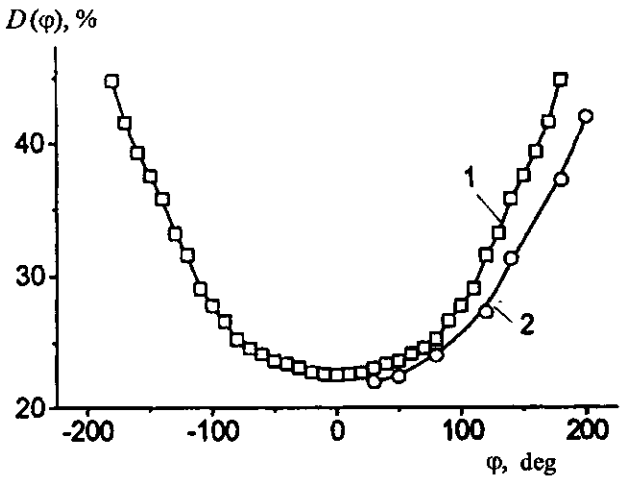

Fig. 3

Local efficiency function for the ring-shaped scintillation detector: (*1*) mathematical modeling, (*2*) experiment.

We have also calculated for the given scintillation detector the relationship between the integrated detection efficiency and the value of r_0 at $R_0 = 50$ mm. It has been found that at $r_0/R_0 > 0.1$ the efficiency starts dropping substantially. This result is of interest, for, in both the commercially available and laboratory scintillation detectors used today, the ratio r_0/R_0 is around 0.2. At the same time, in back-scattered electron spectrometers the lower bound on the ratio r_0/R_0 is governed by the design of the exit slit and usually comes to 0.05–0.01. So, the size of such spectrometers can be reduced without any loss of the detection efficiency by decreasing r_0 at a given R_0.

Figure 4*a* (curve *2*) presents the function $D = D(x, z)$ along the line passing parallel to the x-axis (the coordinate system is shown in Fig. 1*a*) at a distance of 10 mm from the edge of the Robinson detector. Figure 4*b* (curve *2*) shows a similar function in the case where the point M moves from the origin of coordinates to the exit light guide along the z-axis. When calculating these functions, no account has been taken of the hole for the SEM electron probe. It can be seen from the data presented that the efficiency of that part of the detector which is most distant from the exit light guide (beginning at the hole for the electron probe) is materially lower than that of the region adjacent to the light guide. The removal of this part reduces but insignificantly the integrated detection efficiency. The size of the scintillation detector is in that case reduced substantially and its compatibility with other types of detectors, e. g., X-ray detectors, is improved.

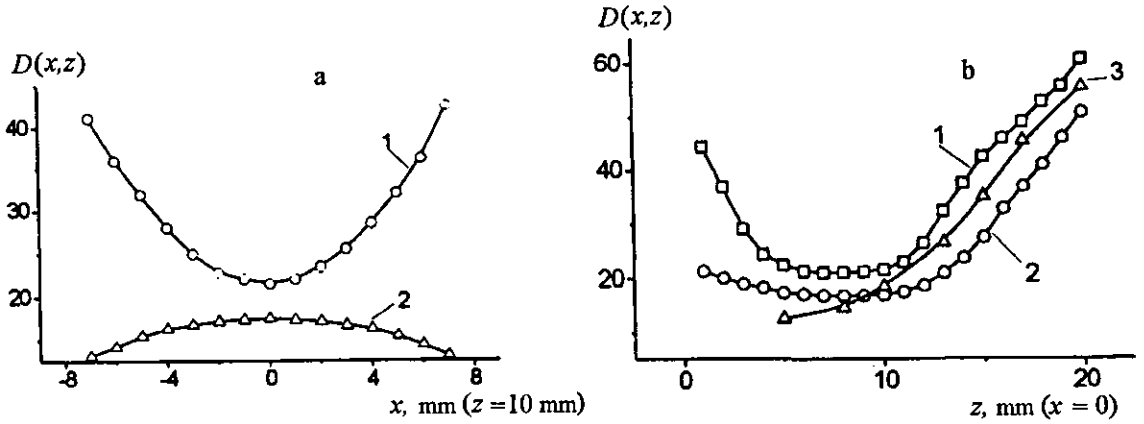

Fig. 4

Local efficiency function for (*a*) the Robinson detector and (*b*) modified scintillation detector in the shape of an elliptic paraboloid. For curve designations, see text.

On retention of the scintillation detector overall dimensions, the integrated detection efficiency can be substantially increased by changing the detector optical part shape. We have suggested [15] that the Robinson detector optical part be made in the shape of an elliptic paraboloid whose surface is described by the equation $x^2/p + y^2/q = 2z$, where p and q are related to the semiaxes a and b of the elliptic cross section at $z = z_0$ as $a = (2pz_0)^{1/2}$ and $b = (2qz_0)^{1/2}$. Such a detector similar in size to the Robinson detector considered above should have the parameters $a = 20$ mm and $b = 5$ mm in the section $z_0 = 20$ mm (Fig. 1*b*). Curves *1* in Fig. 4*a* and *b* are calculated for the case of elliptic paraboloid under the same conditions as in the case of the Robinson detector. It can be seen from the data presented that the peripheral regions of the detector contribute materially to its integrated efficiency. Changing the shape of the scintillation detector results in a partial focusing of radiation within the optical part of the detector, a substantial reduction of the number of repeated internal reflections, and a shortening of the average trajectory length. The above change of the detector shape allows one to make effective that part of the detector which is most remote from the photodetector. The integrated efficiency of the detector suggested is approximately five times that of the standard detectors of comparable size.

CONCLUSION

The results obtained point to a great nonuniformity of the detection capacity of the active part of wide-aperture scintillation back-scattered electron detectors and detectors of special shape. The physical reason for this nonuniformity is the loss of radiation in the light transport inside the scintillation detector. Because of this phenomenon, namely, the nonuniform radiation loss, the design of most scintillation detectors used in SEMs proves not optimal. The suggested modification of the shape of the optical part of the standard Robinson detector has improved its integrated detection efficiency five times. The analysis performed by the

method suggested for modeling the light transport efficiency has shown that the efficiency of the standard detectors amounts, as a rule, to 50–60% of the possible value.

The existence of the effect detected necessitates a critical revision of the existing algorithms for the quantitative processing of information under back-scattered electron detection conditions in scanning electron microscopy.

This work was supported by the Russian Foundation for Basic Research (Grant 98-02-16999) and INTAS (Grant 97-31864).

REFERENCES

1. Z.J. Radzimski and J.C. Russ, *Scanning*, vol. 16, p. 276, 1994.
2. D. Kaczmarek, Z. Czyzewski, I. Hejna, and Z.J. Radzimski, *Scanning*, vol. 9, p. 109, 1987.
3. V.V. Aristov, V.V. Kazmiruk, N.G. Ushakov, and A.A. Firsova, *Poverkhnost'. Fizika, Khimiya, Mekhanika*, no. 4, p. 120, 1989.
4. V.V. Aristov, E.I. Rau, and E.B. Yakimov, *Phys. Stat. Solidi (a)*, vol. 150, p. 211, 1995.
5. E.I. Rau and V.N.E. Robinson, *Scanning*, vol. 18, p. 556, 1996.
6. V.N.E. Robinson, *J. Phys. E.: Sci. Instr.*, vol. 2, p. 650, 1974.
7. J. Hejna, *Scanning*, vol. 17, p. 387, 1995.
8. M. Lange, L. Reimer, and C. Tollkamp, *J. Microscopy*, vol. 134, p. 1, 1984.
9. M. Born, E. Wolf, *Fundamentals of Optics* (Russian translation), Moscow, 1973.
10. C. Carrier and R. Lecomte, *Nucl. Instr. Meth. Phys. Res.*, vol. A292, p. 685, 1990.
11. A.V. Gostev, N.N. Dremova, E.I. Rau, et al., *Izv. Ross. Akad. Nauk, Ser. Fiz.*, vol. 61, p. 1996, 1997.
12. F. Falk and P. Sparrman, *Nucl. Instr. Meth. Phys. Res.*, vol. 85, p. 253, 1970.
13. Y. Xiaoguang, *Nucl. Instr. Meth. Phys. Res.*, vol. 228, p. 101, 1984.
14. P. Schauer and R. Autrata, *Scanning*, vol. 14, p. 325, 1992.
15. R.N. Birchenko, M.N. Filippov, E.I. Rau, et al., *Proc. 14th Int. Conf. on Electron Microscopy*, Cancun, Mexico, vol. 1, p. 77, 1998.

31 March 1999

Department of Physical Electronics